

A Novel Q-stem Connected Architecture for Beyond-Diagonal Reconfigurable Intelligent Surfaces

Xiaohua Zhou[‡], Tianyu Fang[†], Yijie Mao[‡]

[‡]School of Information Science and Technology, ShanghaiTech University, Shanghai 201210, China

[†]Centre for Wireless Communications, University of Oulu, Finland

Email:{zhouxh3, maoyj}@shanghaitech.edu.cn, tianyu.fang@oulu.fi

Abstract—Beyond-diagonal reconfigurable intelligent surface (BD-RIS) has garnered significant research interest recently due to its ability to generalize existing reconfigurable intelligent surface (RIS) architectures and provide enhanced performance through flexible inter-connection among RIS elements. However, current BD-RIS designs often face challenges related to high circuit complexity and computational complexity, and there is limited study on the trade-off between system performance and circuit complexity. To address these issues, in this work, we propose a novel BD-RIS architecture named Q-stem connected RIS that integrates the characteristics of existing single connected, tree connected, and fully connected BD-RIS, facilitating an effective trade-off between system performance and circuit complexity. Additionally, we propose two algorithms to design the RIS scattering matrix for a Q-stem connected RIS aided multi-user broadcast channels, namely, a low-complexity least squares (LS) algorithm and a suboptimal LS-based quasi-Newton algorithm. Simulations show that the proposed architecture is capable of attaining the sum channel gain achieved by fully connected RIS while reducing the circuit complexity. Moreover, the proposed LS-based quasi-Newton algorithm significantly outperforms the baselines, while the LS algorithm provides comparable performance with a substantial reduction in computational complexity.

Index Terms—Beyond-diagonal reconfigurable intelligent surface (BD-RIS), scattering matrix design.

I. INTRODUCTION

Reconfigurable intelligent surface (RIS) has emerged as a pivotal technology for advancing 6G networks. By incorporating multiple passive and reconfigurable elements to manipulate signal direction and intensity, RIS significantly enhances received signal quality, thereby improving overall network performance and facilitating the realization of ambitious 6G goals [1]. Recently, beyond-diagonal RIS (BD-RIS) has been proposed in [2] as a pioneering RIS architecture that generalizes conventional diagonal RIS. Pursuant to the microwave theory, BD-RIS introduces a beyond-diagonal scattering matrix (also known as passive beamforming matrix), allowing for interconnections among its elements.

This work has been supported in part by the National Nature Science Foundation of China under Grant 62201347; and in part by Shanghai Sailing Program under Grant 22YF1428400. The work of Tianyu Fang was supported by the Research Council of Finland through 6G Flagship under Grant 346208 and through project DIRECTION under Grant 354901. (Corresponding author: Yijie Mao)

According to different interconnection architectures, BD-RIS can be categorized into: single, fully, and group connected architectures [3]. Specifically, single connected RIS [4] refers to the conventional diagonal RIS configuration where each RIS element is connected to a single load or impedance network. In this architecture, each RIS element operates independently, allowing for phase adjustments but limiting the inter-element interactions. Fully connected RIS [2] refers to an architecture in which every RIS element is interconnected with all other elements. This means that each RIS port can communicate with all other ports, allowing for maximum flexibility in controlling the phase and amplitude of the reflected signals. To reduce the circuit complexity, group connected RIS is introduced in [2]. It assigns the RIS elements into defined groups where only the elements within each group are interconnected, creating a block diagonal susceptance matrix that allows for independent control and optimization of each group while reducing overall circuit complexity. Moreover, a tree connected architecture is introduced in [5] based on graph theory. By employing a tree graph, tree connected RIS further enhances the trade-off between performance and circuit complexity. Besides, simultaneously transmitting and reflecting RIS (STAR-RIS) [6] and multi-sector BD-RIS [7] are advanced types of RIS that differ from the aforementioned RIS by allowing signals to be both reflected and transmitted through the surface. In this paper, we focus on BD-RIS within reflect mode only.

Among all the aforementioned BD-RISs, the fully connected BD-RIS enables all elements to connect with each other, thereby achieving the maximum performance gain, albeit at the cost of the highest circuit complexity. Group connected RIS significantly reduces circuit complexity but suffers from performance degradation, failing to achieve an optimal trade-off between channel gain performance and circuit complexity. Although tree connected RIS has been shown to be the simplest BD-RIS architecture for achieving the optimal performance in single-user multiple-input single-output (MISO) [5], its performance in multi-user MISO remains unexplored.

Based on these literature, this paper aims to further enhance the trade-off between the channel gain performance and circuit complexity. To this end, we propose a brand-new BD-RIS architecture, named Q-stem connected RIS for multi-user downlink transmission networks. This structure

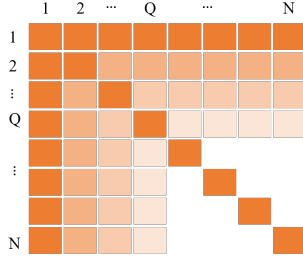


Fig. 2: The shape of a feasible susceptance matrix \mathbf{B} for Q-stem connected RIS. The non-zero elements in \mathbf{B} are represented in orange.

the degree of the vertices in $\mathcal{V}_{\bar{Q}}$ is Q , as depicted in Fig. 1b. In Fig. 2, we further illustrate a feasible susceptance matrix \mathbf{B} for Q-stem connected RIS which satisfies the constraint in (5), i.e., $\mathbf{B} \in \mathcal{B}_Q$. All non-zero elements in \mathbf{B} are represented in orange color. Obviously, \mathbf{B} has in total $(2N - 1)Q - Q^2$ non-zero off-diagonal entries.

C. Connection Between Q-stem Connected RIS and Other RIS Architectures

Q-stem connected RIS is a general BD-RIS architecture which bridges existing single connected RIS, tree connected RIS, and fully connected RIS by adjusting the parameter Q . Specifically,

- When $Q = 0$, the proposed Q-stem connected RIS reduces to a single connected RIS, the corresponding graph is empty. The susceptance matrix \mathbf{B} reduces to:

$$\mathbf{B} = \text{diag}([\mathbf{B}]_{11}, \dots, [\mathbf{B}]_{NN}). \quad (6)$$

- When $Q = 1$, the proposed Q-stem connected RIS is equivalent to a tree connected RIS. Its graph becomes a tree. The susceptance matrix \mathbf{B} for tree connected RIS becomes

$$\mathbf{B} = \mathbf{B}^T, \mathbf{B} \in \mathcal{B}_G, \quad (7)$$

where $\mathcal{B}_G = \{\mathbf{B} | [\mathbf{B}]_{n,m} = 0, n \neq m, m > 1, n > 1\}$.

- When $Q = N - 1$, the proposed Q-stem connected RIS becomes a fully connected RIS, where the graph is complete. In this case, all ports are interconnected via tunable impedance components, offering maximum design flexibility and performance [2].

D. Circuit Complexity of Q-Stem Connected RIS

The circuit topology complexity is reflected in the number of independent tunable admittance components, which corresponds to the number of independent variables in the symmetric susceptance matrix \mathbf{B} . Q-stem connected RIS includes N admittance components connecting each port to ground and $QN - Q(Q + 1)/2$ admittance components interconnecting the ports to each other, yielding a total of $QN + N - Q(Q + 1)/2$ admittance components. Table I provides the circuit complexity comparison among various architectures for BD-RIS. Notably, the circuit complexity of Q-stem connected RIS scales linearly with the number of elements for a fixed Q .

TABLE I: Circuit Complexity Comparison for Different RIS Architectures.

Architecture	Reference	Circuit Complexity
Single connected RIS	[4]	N
Group connected RIS	[2]	$N(N/G + 1)/2$
Fully connected RIS	[2]	$N(N + 1)/2$
Tree connected RIS	[5]	$2N - 1$
Q-Stem connected RIS	Proposed	$QN + N - Q(Q + 1)/2$

E. Problem Formulation

To show the effectiveness of our proposed Q-stem connected RIS, we next design its scattering matrix Θ with the aim of maximizing the sum channel gains among users. The formulated problem is given as:

$$\max_{\Theta} \|\mathbf{H}^H \Theta \mathbf{E}\|_F^2 \quad (8a)$$

$$\text{s. t. } \Theta = (\mathbf{I} + jZ_0 \mathbf{B})^{-1} (\mathbf{I} - jZ_0 \mathbf{B}), \quad (8b)$$

$$\mathbf{B} = \mathbf{B}^T, \quad (8c)$$

$$\mathbf{B} \in \mathcal{B}_Q, \quad (8d)$$

where $\|\cdot\|_F$ denotes the Frobenius Norm. Problem (8) is challenging to solve since constraint (8b) is highly non-convex. Although the passive beamforming design to maximize the channel gain has been developed for fully connected RIS [10], [11], tree connected RIS [5] and group connected RIS [12], they cannot be applied to address the problem for our proposed Q-stem connected RIS due to its unique scattering matrix constraint. Specifically, the algorithm in [5], [10], [12] focus in single-user transmission networks while [11] only address fully connected RIS configurations. To the best of our knowledge, no existing algorithms proposed for BD-RIS can be directly applied to solve it. In the next section, we will propose an efficient algorithm to address this problem.

III. PROPOSED EFFICIENT ALGORITHM

In this section, we first analyze an upper bound of the sum channel gains for problem (8). Based on such upper bound, we then propose a closed-form solution to problem (8).

A. Theoretical Upper Bound Analysis for Problem (8)

In this subsection, we first relax problem (8) by removing constraints (8c) and (8d). Then, we apply singular value decomposition (SVD) to \mathbf{H}^H and \mathbf{E} , i.e., $\mathbf{H}^H = \mathbf{U}\mathbf{S}\mathbf{V}^H$ and $\mathbf{E} = \mathbf{P}\Sigma\mathbf{W}^H$, where $\mathbf{S} \in \mathbb{R}^{K \times N}$, $\Sigma \in \mathbb{R}^{N \times L}$, and $\mathbf{U} \in \mathbb{C}^{K \times K}$, $\mathbf{V} \in \mathbb{C}^{N \times N}$, $\mathbf{P} \in \mathbb{C}^{N \times N}$, $\mathbf{W} \in \mathbb{C}^{L \times L}$ are unitary matrices. The relaxed problem is obtained as:

$$\max_{\Theta} \|\mathbf{U}\mathbf{S}\mathbf{V}^H \Theta \mathbf{P}\Sigma\mathbf{W}^H\|_F^2 \quad (9a)$$

$$\text{s. t. } \Theta \Theta^H = \mathbf{I}_N. \quad (9b)$$

Problem (9) is also a relaxed formulation of the sum channel gain maximization problem for fully connected RIS, where the symmetric constraint $\Theta = \Theta^T$ is relaxed. Since $\mathbf{U}\mathbf{U}^H = \mathbf{I}_K$ and $\mathbf{W}\mathbf{W}^H = \mathbf{I}_L$, the objective function of problem (9) is equivalent to $\|\mathbf{S}\mathbf{V}^H \Theta \mathbf{P}\Sigma\|_F^2$. To obtain more insights of the channel shaping capability of BD-RIS, we introduce the following definition.

Definition 2. (Degree of freedom) The degree of freedom (DoF), also known as multiplexing gain, is the maximum number of independent streams transmitted in parallel over a MIMO channel. The DoF for the compact effective channels $\mathbf{F} \triangleq [\mathbf{f}_1, \dots, \mathbf{f}_K] \in \mathbb{C}^{L \times K}$ is defined as [13]

$$M = \lim_{\rho \rightarrow \infty} \frac{\log \det (\mathbf{I}_L + \rho \mathbf{F} \mathbf{F}^H)}{\log \rho} = \min(K, L, N), \quad (10)$$

where ρ is the signal-to-noise ratio (SNR).

Based on the definition of DoF M in Definition 2, we then partition the matrices \mathbf{V} and \mathbf{P} as $\mathbf{V} = [\mathbf{V}_M, \mathbf{V}_{N-M}]$ and $\mathbf{P} = [\mathbf{P}_M, \mathbf{P}_{N-M}]$. We also partition \mathbf{S} and $\mathbf{\Sigma}$ as $\mathbf{S} = \text{diag}(\mathbf{S}_M, \mathbf{S}_{K-M})$ and $\mathbf{\Sigma} = \text{diag}(\mathbf{\Sigma}_M, \mathbf{\Sigma}_{L-M})$. In this way, we have

$$\begin{aligned} \|\mathbf{S} \mathbf{V}^H \mathbf{\Theta} \mathbf{P} \mathbf{\Sigma}\|_F^2 &= \|\mathbf{S}_M \mathbf{V}_M^H \mathbf{\Theta} \mathbf{P}_M \mathbf{\Sigma}_M\|_F^2 \\ &\stackrel{(a)}{\leq} \|\mathbf{S}_M \mathbf{\Sigma}_M\|_F^2, \end{aligned} \quad (11)$$

where the equality in (a) holds if and only if

$$\mathbf{V}_M^H \mathbf{\Theta} \mathbf{P}_M = \mathbf{\Phi}, \quad (12)$$

and $\mathbf{\Phi} = \text{diag}([e^{j\phi_1}, \dots, e^{j\phi_M}])$ with $\phi_m \in [0, 2\pi)$, $m = 1, \dots, M$. This is a sufficient condition to achieve the theoretic upper bound of problem (8). This upper bound can provide more insights in channel rearrangement and channel space alignment, and more details are provided in [13]. However, it is worth noting that, limited by the physical reciprocal property, i.e., $\mathbf{\Theta} = \mathbf{\Theta}^T$, all BD-RIS structures can not attain this theoretical upper bound in most cases as shown in the following Proposition 1.

Proposition 1. Fully connected RIS can not achieve the performance upper bound in (11) when the DoF for the compact effective channels \mathbf{F} is larger than 1, i.e., $M > 1$. It only achieves the performance upper bound when $M = 1$.

Proof. See Appendix. ■

Since fully connected RIS offers the highest design flexibility among BD-RIS structures and cannot achieve the upper bound in (11) when $M > 1$, neither can any other BD-RIS structures, including Q-stem connected RIS.

B. Proposed Least Square-based Algorithms for Problem (8)

Through the analysis in the last subsection, we obtain that the upper bound in (11) for problem (8) cannot be achieved by Q-stem connected RIS. As the upper bound (11) is guaranteed to be achieved by the sufficient condition (12), we therefore obtain an upper bound of problem (8) by replacing its objective function (8a) with (12), which is given as

$$(12), (8b), (8c), (8d). \quad (13)$$

Following our discussion in Section III-A, by relaxing constraint (8d) in (13), we obtain problem (25) in the appendix for fully-connected RIS. Such problem has no solution when $M > 1$. Therefore, (13) has no solution when $M > 1$ either due to the additional constraint (8d). In the following, we propose a least square (LS) method for solving (13).

Before delving into the LS solution, we first introduce a novel vectorization operator.

Definition 3. (Independent Vectorization) For any matrix \mathbf{B} , the operator $\text{vec}_i(\mathbf{B})$ is used to extract all independent variables from \mathbf{B} and convert them into a vector.

For our proposed Q-stem connected RIS, there are $QN + N - Q(Q+1)/2$ independent variables in \mathbf{B} as per Fig. 2. Therefore, the independent vectorization of \mathbf{B} is given as

$$\begin{aligned} \text{vec}_i(\mathbf{B}) &= [[\mathbf{B}]_{1,1}, \dots, [\mathbf{B}]_{1,N}, \dots, [\mathbf{B}]_{Q,Q}, \dots, [\mathbf{B}]_{Q,N}, \\ &[\mathbf{B}]_{Q+1,Q+1}, \dots, [\mathbf{B}]_{N,N}]^T \in \mathbb{R}^{(QN+N-\frac{Q(Q+1)}{2}) \times 1}. \end{aligned} \quad (14)$$

It is worth noting that the independent vectorization $\text{vec}_i(\mathbf{B})$ is a linear transformation of the conventional vectorization operator $\text{vec}(\mathbf{B})$ which simply stacks the columns of \mathbf{B} on top of one another. Specifically, by defining $\mathbf{R} \in \mathbb{R}^{N^2 \times (QN+N-\frac{Q(Q+1)}{2})}$ as a transformation matrix and $\mathbf{b} \triangleq \text{vec}_i(\mathbf{B})$, we have

$$\text{vec}(\mathbf{B}) = \mathbf{R} \mathbf{b}, \quad (15)$$

where \mathbf{R} is used to map \mathbf{b} to $\text{vec}(\mathbf{B})$ so as to satisfy the Q-stem connected RIS constraints $\mathbf{B} \in \mathcal{B}_Q$ and $\mathbf{B} = \mathbf{B}^T$. The elements of \mathbf{R} are either 0 or 1.

Next, we use $\mathbf{b} \triangleq \text{vec}_i(\mathbf{B})$ to obtain our proposed LS method. Specifically, we first substitute (8b) into (12) and equivalently rewrite (12) as

$$\mathbf{B} \mathbf{C} = \mathbf{D}, \quad (16)$$

where $\mathbf{C} = jZ_0(\mathbf{V}_M + \mathbf{P}_M) \in \mathbb{C}^{N \times M}$ and $\mathbf{D} = \mathbf{P}_M - \mathbf{V}_M \in \mathbb{C}^{N \times M}$. Since \mathbf{B} is a real-value matrix, we could further transform (16) into real and imaginary equations, which is given as

$$\mathbf{B} \Re\{\mathbf{C}\} = \Re\{\mathbf{D}\}, \quad \mathbf{B} \Im\{\mathbf{C}\} = \Im\{\mathbf{D}\}, \quad (17)$$

where $\Re(\cdot)$ and $\Im(\cdot)$ respectively denote the real and imaginary parts of a complex matrix.

By applying the conventional vectorization operator to both sides of (17), (17) can be equivalently transformed into

$$(\Re\{\mathbf{C}\}^T \otimes \mathbf{I}_N) \text{vec}(\mathbf{B}) = \text{vec}(\Re\{\mathbf{D}\}), \quad (18a)$$

$$(\Im\{\mathbf{C}\}^T \otimes \mathbf{I}_N) \text{vec}(\mathbf{B}) = \text{vec}(\Im\{\mathbf{D}\}), \quad (18b)$$

where \otimes represents the Kronecker product. We further substitute (15) into (18) and obtain

$$(\Re\{\mathbf{C}\}^T \otimes \mathbf{I}_N) \mathbf{R} \mathbf{b} = \text{vec}(\Re\{\mathbf{D}\}), \quad (19a)$$

$$(\Im\{\mathbf{C}\}^T \otimes \mathbf{I}_N) \mathbf{R} \mathbf{b} = \text{vec}(\Im\{\mathbf{D}\}). \quad (19b)$$

By combining (19a) and (19b), we equivalently transform the problem (13) into a linear equation of \mathbf{b} given as:

$$\mathbf{A} \mathbf{b} = \mathbf{z}, \quad (20)$$

where $\mathbf{A} = [(\Re\{\mathbf{C}\}^T \otimes \mathbf{I}_N) \mathbf{R}; (\Im\{\mathbf{C}\}^T \otimes \mathbf{I}_N) \mathbf{R}] \in \mathbb{R}^{2MN \times (\frac{2N-1}{2}Q - \frac{Q^2}{2} + N)}$, $\mathbf{z} = [\text{vec}(\Re\{\mathbf{D}\}); \text{vec}(\Im\{\mathbf{D}\})] \in \mathbb{R}^{2MN \times 1}$.

Due to the equivalence between (13) and (20), equation

Algorithm 1: Proposed least spare (LS) solution for problem (8)

- 1 **Input:** The channel matrices \mathbf{H}^H and \mathbf{E} ;
 - 2 Obtain \mathbf{V} and \mathbf{P} through SVD decomposition;
 - 3 Obtain \mathbf{V}_M and \mathbf{P}_M defined in (11);
 - 4 Obtain \mathbf{R} , \mathbf{C} and \mathbf{D} defined in (15) and (16);
 - 5 Obtain \mathbf{A} and \mathbf{z} defined in (20);
 - 6 Obtain $\mathbf{b} = (\mathbf{A}^T \mathbf{A})^{-1} \mathbf{A}^T \mathbf{z}$;
-

(20) has no solution when $M > 1$. Therefore, we propose to employ the LS solution to solve equation (20) as closely as possible. Following the fundamentals of LS solution in [14], we obtain the LS solution for (20), which is given as:

$$\mathbf{b} = (\mathbf{A}^T \mathbf{A})^{-1} \mathbf{A}^T \mathbf{z}. \quad (21)$$

The details of our proposed LS method is illustrated in Algorithm 1. The computational complexity of Algorithm 1 is dominated by Step 6, which has the order of $\mathcal{O}(Q^3 N^3)$.

It is worth noting that our proposed LS method is an efficient closed-form solution. As such, it can be effectively utilized as a good initialization point for the quasi-Newton method [2], [15], which is a typical approach to solve unconstrained optimization problems. In our proposed LS-based quasi-Newton algorithm, the scattering matrix is first initialized by Algorithm 1 with $\text{vec}(\mathbf{B}) = \mathbf{R}\mathbf{b}$. This is then followed by applying the quasi-Newton method to address the following problem:

$$\max_{\mathbf{b}} \|\mathbf{H}^H (\mathbf{I} + jZ_0 \mathbf{B})^{-1} (\mathbf{I} - jZ_0 \mathbf{B}) \mathbf{E}\|_F^2 \quad (22)$$

IV. SIMULATION RESULTS

In this section, we evaluate the simulation results of the proposed Q-stem connected RIS architecture and the LS algorithm for solving the sum channel gain maximization problem. We assume that the distances between the BS and the RIS, and between the RIS and users are both $50\sqrt{2}$ meters. The path loss follows the model $P(d) = L_0 d^{-\alpha}$, where $L_0 = -30$ dB represents the reference path loss at $d = 1$ m, d is the link distance, and α is the path loss exponent. Following [15], the path loss exponents for the BS-RIS and RIS-user links are set to 2 and 2.2, respectively. The small-scale fading model is based on Rayleigh fading. All simulation results are averaged over 100 random channel realizations. The following five schemes are compared in this work:

- *Newton-LS, Q-stem:* This refers to the quasi-Newton method initialized with our proposed LS method for Q-stem connected RIS.
- *Newton-random, Q-stem:* This refers to the quasi-Newton method initialized with a random scattering matrix for Q-stem connected RIS.
- *Newton-LS, fully:* This refers to the quasi-Newton method initialized with our proposed LS method for fully connected RIS, i.e., $Q = N - 1$.
- *Upper bound:* This refers to the upper bound $\|\mathbf{S}_M \mathbf{\Sigma}_M\|_F$ in (11).

- *LS, Q-stem:* This refers to our proposed LS method in Algorithm 1 for Q-stem connected RIS.

For the proposed Q-stem connected RIS, it simplifies to a single connected RIS when $Q = 0$, and to tree connected RIS when $Q = 1$.

In Fig. 3, we show the channel gain versus the value of Q in susceptance matrix \mathbf{B} with $N = 64$. While the fully connected RIS is close to achieving upper bound performance, it does not reach it. As Q increases, the proposed LS solution approaches more closely the sum channel gain achieved by the optimal solution specified in (8). Algorithmically, the proposed low-complexity LS method achieves worse sum channel gain than the our proposed Newton-LS method for small Q . However, as Q increases, the gap narrows, and at $Q = 7$, both methods yield identical performance. Additionally, our proposed Newton-LS method surpasses the Newton-random approach thanks to a better initialization achieved by our proposed LS algorithm.

In Fig. 4, the sum channel gain performance of LS and Newton-LS method is illustrated with different number of BD-RIS elements when $L = K = 4$. As N increases, the performance of fully connected RIS, Q-stem connected RIS, and the upper bound all improve. Additionally, the performance of the LS method enhances with increasing Q . Specifically, when $Q = 7$, the LS method matches the performance of the Newton-LS method. While neither the fully connected RIS nor the Q-stem connected RIS at $Q = 7$ reaches the upper bound, but both demonstrate performance comparable to it.

Fig. 5 illustrates the sum channel gain performance of the Newton-LS method as the number of the streams M increases when $L = 5$. Given that $K \leq L$, we have $M = K$ in this case. As M grows, the channel gain improves for all BD-RIS architectures. Notably, when $Q = 2M - 1$, Q-stem connected RIS matches the performance of fully connected RIS.

V. CONCLUSION

In this paper, we propose a novel Q-stem connected RIS architecture for a downlink BD-RIS-assisted multi-user MISO transmission network, aiming at balancing system performance and RIS circuit complexity. Based on the proposed Q-stem connected RIS, we address its sum channel gain maximization problem by proposing a low-complexity LS algorithm to design its scattering matrix, along with a Newton-based algorithm utilizing our proposed LS solution for initialization. Numerical results demonstrate that our proposed Q-stem connected RIS significantly reduces circuit complexity while maintaining comparable performance to other baseline schemes for some Q values. Furthermore, the LS method achieves the same performance as fully connected RIS when Q reaches a specific threshold, and the proposed LS-based Newton-based algorithm outperforms other baseline methods significantly. Thus, we conclude that the Q-stem connected RIS and LS algorithm offer substantial potential for practical BD-RIS applications.

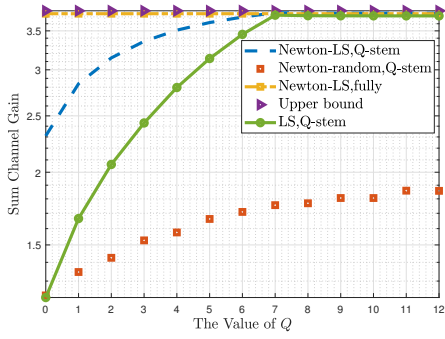


Fig. 3: Channel gain versus the value of Q in \mathbf{B} when $L = K = 4$ and $N = 64$.

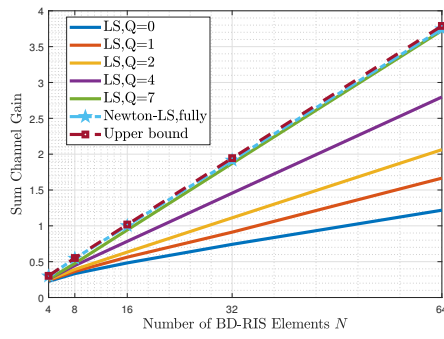


Fig. 4: Channel gain versus the number of BD-RIS elements when $L = K = 4$.

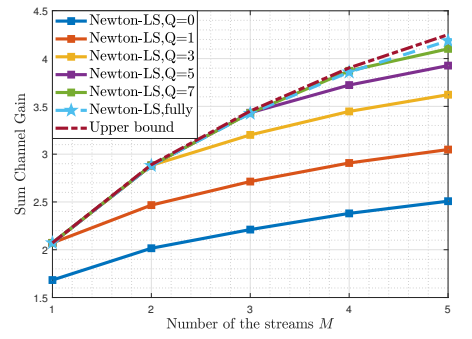


Fig. 5: Channel gain versus the number of streams when $L = 5$ and $N = 64$.

APPENDIX

When considering a fully connected RIS, i.e., $Q = N - 1$, problem (8) reduces to

$$\max_{\Theta} \|\mathbf{S}_M \mathbf{V}_M^H \Theta \mathbf{P}_M \Sigma_M\|_F^2 \quad (23a)$$

$$\text{s. t. } \Theta \Theta^H = \mathbf{I}_N, \Theta = \Theta^T. \quad (23b)$$

Similar to the analysis of problem (9), the theoretical upper bound of problem (23) can be achieved if and only if the following equation set has solution

$$\mathbf{V}_M^H \Theta \mathbf{P}_M = \Phi, \quad (24a)$$

$$\Theta \Theta^H = \mathbf{I}_N, \quad (24b)$$

$$\Theta = \Theta^T. \quad (24c)$$

The solution of (24a) and (24b) is given by

$$\Theta^* = \mathbf{V}_M \Phi \mathbf{P}_M^H + \mathbf{V}_{N-M} \mathbf{X} \mathbf{P}_{N-M}^H, \quad (25)$$

where \mathbf{X} is an unitary matrix. Without loss of generality, we set $\phi_m = 0$ in the following discussion, as its value does not affect the final objective value. The equation set (24) can be further simplified as

$$\Theta = \mathbf{V}_M \mathbf{P}_M^H + \mathbf{V}_{N-M} \mathbf{X} \mathbf{P}_{N-M}^H, \Theta = \Theta^T. \quad (26)$$

When considering the special case $M = 1$, (26) has solutions as shown in [10], [12]. Next, we prove by contradiction that when $M > 1$, (26) has no solution.

Assume that there exists at least one solution of (26), we have

$$\mathbf{V}_M \mathbf{P}_M^H + \mathbf{V}_{N-M} \mathbf{X} \mathbf{P}_{N-M}^H = \mathbf{P}_M^* \mathbf{V}_M^T + \mathbf{P}_{N-M}^* \mathbf{X}^H \mathbf{V}_{N-M}^T. \quad (27)$$

By left multiplying \mathbf{V}_M^H and right multiplying \mathbf{V}_M^* to (27), we have

$$\mathbf{P}_M^H \mathbf{V}_M^* = \mathbf{V}_M^H \mathbf{P}_M^*. \quad (28)$$

Let $\Lambda \triangleq \mathbf{P}_M^H \mathbf{V}_M^* \in \mathbb{C}^{M \times M}$, we have $\Lambda = \Lambda^T$. When $M = 1$, $\Lambda \in \mathbb{C}$ is a constant scalar, so that $\Lambda = \Lambda^T$ holds obviously. However, when $M > 1$, Λ is not symmetric with probability 1 because \mathbf{V}_M and \mathbf{P}_M are unitary matrices from the SVD of \mathbf{H}^H and \mathbf{E} , respectively. This contradicts our initial assumption. Therefore, when $M > 1$, no solution for (24) exists. Hence, when $M > 1$, fully connected RIS cannot

achieve the theoretical upper bound performance, completing the proof for the proposition.

REFERENCES

- [1] Q. Wu and R. Zhang, "Towards smart and reconfigurable environment: Intelligent reflecting surface aided wireless network," *IEEE Commun. Mag.*, vol. 58, no. 1, pp. 106–112, Jan 2020.
- [2] S. Shen, B. Clerckx, and R. Murch, "Modeling and architecture design of reconfigurable intelligent surfaces using scattering parameter network analysis," *IEEE Trans. Wireless Commun.*, vol. 21, no. 2, pp. 1229–1243, Feb. 2022.
- [3] H. Li, S. Shen, and B. Clerckx, "Beyond diagonal reconfigurable intelligent surfaces: From transmitting and reflecting modes to single-, group- and fully-connected architectures," *IEEE Trans. Wireless Commun.*, vol. 22, no. 4, pp. 2311–2324, Apr. 2023.
- [4] Q. Wu and R. Zhang, "Intelligent reflecting surface enhanced wireless network via joint active and passive beamforming," *IEEE Trans. Wireless Commun.*, vol. 18, no. 11, pp. 5394–5409, Nov. 2019.
- [5] M. Nerini, S. Shen, H. Li, and B. Clerckx, "Beyond diagonal reconfigurable intelligent surfaces utilizing graph theory: Modeling, architecture design, and optimization," *IEEE Trans. Wireless Commun.*, vol. 23, no. 8, pp. 9972–9985, Aug. 2024.
- [6] J. Xu, Y. Liu, X. Mu, and O. A. Dobre, "STAR-RISs: Simultaneous transmitting and reflecting reconfigurable intelligent surfaces," *IEEE Commun. Lett.*, vol. 25, no. 9, pp. 3134–3138, Sep. 2021.
- [7] H. Li, S. Shen, and B. Clerckx, "Beyond diagonal reconfigurable intelligent surfaces: A multi-sector mode enabling highly directional full-space wireless coverage," *IEEE J. Sel. Areas Commun.*, vol. 41, no. 8, pp. 2446–2460, Aug. 2023.
- [8] D. M. Pozar, *Microwave engineering: theory and techniques*. John Wiley & sons, 2021.
- [9] M. Nerini, S. Shen, H. Li, M. D. Renzo, and B. Clerckx, "A universal framework for multiport network analysis of reconfigurable intelligent surfaces," *IEEE Trans. Wireless Commun.*, pp. 1–1, Jun. 2024.
- [10] I. Santamaria, M. Soleymani, E. Jorswieck, and J. Gutiérrez, "SNR maximization in beyond diagonal RIS-assisted single and multiple antenna links," *IEEE Signal Process. Lett.*, vol. 30, pp. 923–926, Jul. 2023.
- [11] T. Fang and Y. Mao, "A low-complexity beamforming design for beyond-diagonal RIS aided multi-user networks," *IEEE Commun. Lett.*, Jan. 2024.
- [12] M. Nerini, S. Shen, and B. Clerckx, "Closed-form global optimization of beyond diagonal reconfigurable intelligent surfaces," *IEEE Trans. Wireless Commun.*, Feb. 2024.
- [13] Y. Zhao, H. Li, M. Franceschetti, and B. Clerckx, "Channel shaping using beyond diagonal reconfigurable intelligent surface: Analysis, optimization, and enhanced flexibility," *arXiv preprint arXiv:2407.15196*, 2024.
- [14] Å. Björck, "Least squares methods," *Handbook of numerical analysis*, vol. 1, pp. 465–652, 1990.
- [15] T. Fang, Y. Mao, S. Shen, Z. Zhu, and B. Clerckx, "Fully connected reconfigurable intelligent surface aided rate-splitting multiple access for multi-user multi-antenna transmission," in *IEEE Int. Conf. Commun. Workshops (ICC Workshops)*, May. 2022, pp. 675–680.